Injection Locking of VCSELs

Chih-Hao Chang, *Student Member, IEEE*, Lukas Chrostowski, *Student Member, IEEE*, and Connie J. Chang-Hasnain, *Fellow, IEEE*

***Abstract*—Injection locking has been actively researched for its possibility to improve laser performance for both digital and analog applications. When a modulated follower laser (also termed "slave" laser) is locked to the master laser, its nonlinear distortion and frequency chirp may be reduced. As well, the resonance frequency can increase to several times higher than its free running case. In this paper, we show that the frequency response (S21) of an injection-locked laser is similar to a parasitic-limited laser with a high resonance frequency. The S21 was studied experimentally and the condition to achieve a flat, enhanced frequency response was identified. For analog applications, a record 112 dB-Hz$^{2/3}$, single-tone third harmonic spur-free dynamic range of a 1.55-μm vertical cavity surface emitting lasers (VCSEL) was demonstrated. An improvement was attained for a wide-injection parameter space. In a 50-km 2.5-Gb/s digital link, a 2-dB power penalty reduction at 10^{-9} bit error rate was also demonstrated. As a novel application, an injection-locked uncooled tunable VCSEL was shown to have a reasonable modulation performance in a wide abient temperature range. The VCSEL was locked to a designated wavelength and the injection compensated the temperature-induced performance degradation. This concept can be extremely attractive for low-cost dense wavelength division muliplexed transmitters.**

***Index Terms*—vertical cavity surface emitting lasers (VCSEL), injection locking, high-frequency modulation, spur-free dynamic range, bit error rate (BER), uncooled laser.**

I. Introduction

INJECTION locking of semiconductor lasers is a research topic that has attracted much interest since the early 1980s. Its applications include receiver end design in optical coherent communication [1], laser spectral narrowing [2], suppression of laser noise [3], the reduction of frequency chirp under modulation [4], and improving the laser intrinsic frequency response [5].

For many applications, the directly modulated laser is unsuitable due to performance issues. In particular, the high-linewidth enhancement factor leads to a high chirp that is undesirable for digital communications. In analog communications, the linearity is not high enough, leading to signal distortion. For both applications, a high-frequency response is desired and may not be met by directly modulated lasers. For the highest capacity systems, designers typically have chosen to incorporate an external modulation device to a continuous-wave (CW) laser. Though this may achieve the desired performance requirements, it does so with the cost of additional system complexity. If possible, a directly modulated laser with higher performance would be ideal. We argue that injection locking gives us the additional design freedom with greatly increased performance that makes injection-locked directly modulated lasers a viable candidate for future analog and digital networks.

The theory of an injection-locked diode laser is discussed in Section II. This model lays out the foundation for both the digital and analog simulations, and is also valuable to gain insight into such a complicated system. Section III focuses on the analog performance of an injection-locked VCSEL. Thorough measurements within the entire locking range, or Arnold tongue, were performed for S21 and for third-order harmonic spur-free dynamic range (SFDR). In Section IV, the first bit error rate (BER) improvement using a low-power, noisy VCSEL as the master laser for a 2.5-GHz directly modulated follower VCSEL is discussed. Simulations also show that injection locking can be useful in realizing a directly modulated VCSEL at 10 Gb/s.

Finally, we demonstrate a novel application of the injection locking technique. The configuration locks an uncooled, tunable VCSEL to a designated wavelength and compensates the performance degradation due to ambient temperature variations. The elimination of the wavelength locker within a transmitter is essential for it to be cost effective. Given a stable multiwavelength master laser source, one single master laser can lock and improve transmitters at different channels simultaneously and reduce the size and cost of the transmitter modules tremendously.

II. Theory of Injection Locking

Starting with the wave equation, the rate equations of an injection-locked laser can be derived as the following [6]:

$$\frac{dS}{dt} = \left[\frac{G_0(N-N_0)}{1+\epsilon S} - \frac{1}{\tau_p}\right] S + 2k_c\sqrt{S\cdot S_{\rm inj}}\cdot\cos\left(\Delta\phi(t)\right) + R_{\rm sp} + F_s \tag{1}$$

$$\frac{d\phi}{dt} = \frac{\alpha}{2}G_0(N-N_{\rm th}) - \Delta\omega + k_c\sqrt{\frac{S_{\rm inj}}{S}}\cdot\sin\left(\Delta\phi(t)\right) + \frac{F_\phi}{S} \tag{2}$$

$$\frac{dN}{dt} = \frac{I}{e} - \frac{N}{\tau_n} - \frac{G_0\left(N-N_0\right)}{1+\epsilon S}\cdot S + F_n. \tag{3}$$

In these equations, $S, \phi,$ and N denote the photon number, the phase, and the carrier number inside the follower laser cavity, respectively. G_0 denotes the gain coefficient, N_0 is the transparency carrier number, τ_p and τ_n are the photon and carrier lifetimes, respectively, I is the follower laser bias current, ϵ is the gain compression factor, and α is the linewidth-enhancement factor. $R_{\rm sp}$ is the spontaneous emission rate and the Langevin

Manuscript received March 4, 2003; revised July 11, 2003. This work was supported by DARPA under Award CSOM F30602-02-2-0096.

The authors are with the Department of Electrical Engineering and Computer Science, University of California, Berkeley, CA 94720 USA (e-mail: hao@photonics.eecs.berkeley.edu).

Digital Object Identifier 10.1109/JSTQE.2003.819510

noise terms F are also added for completeness. For the injection terms, S_{inj} is the injection photon number from the master laser, $\Delta\omega\ (=\omega_{\text{ML}}-\omega_{\text{SL}})$ is the detuning between the two lasers, and $\Delta\phi(t)\ (=\phi_{\text{ML}}(t)-\phi_{\text{SL}}(t))$ is the corresponding phase difference. The coupling coefficient k_c of the master light into the follower laser, is determined by the cavity-round trip time and the reflectivity of the mirror subjected to injection [7]. In our simulations in the later sections, most of the VCSEL parameters are obtained from [8]. In particular, the linewidth-enhancement factor is assumed as five and the gain compression factor is 1.5×10^{-17} cm^3.

Although a VCSEL is intrinsically single longitudinal mode, multiple transverse modes and polarization modes are possible. For the VCSELs used in our experiment, the spectra are highly single mode and the side-mode suppression ratio (SMSR) is >35 dB, even under modulation. The single-mode rate equations (1)–(3) are, thus, a reasonable model to study the injection locking effects.

The follower laser locks to the master only for a certain combination of the injection power and frequency detuning. The stable locking condition can be found as [9]

$$-k_c\sqrt{\frac{S_{\text{inj}}}{S}}\sqrt{1+\alpha^2}<\Delta\omega<k_c\sqrt{\frac{S_{\text{inj}}}{S}}. \tag{4}$$

The presence of the linewidth-enhancement factor makes the follower laser easier to lock to a master laser at the red side and, therefore, the locking range is asymmetric in frequency detuning. Also, a higher injection power results in a larger locking range. If the detuning range is mapped out for different injection powers, we obtain the locking range, or the Arnold tongue, of the system. Similar Arnold tongue structures can be found in many coupled oscillator systems to describe the conditions when the coupled oscillators are synchronized [10]. In our case, when the injection parameters are within the Arnold tongue, the follower laser will lase at the master-laser wavelength, independent of its original lasing wavelength. Note that the stability condition above is valid only when both lasers are biased at CW. The stability condition of a perturbed follower laser can be found in [11].

By performing the small signal analysis of (1)–(3), the modulation response $H(j\omega)$ for the injection locked follower laser can be derived as

$$H(\Omega)=A\cdot\frac{\Omega+p_0}{\Omega^3+q_2\,\Omega^2+q_1\,\Omega+q_0}. \tag{5}$$

In this equation, Ω is used to replace $j\omega$ and the coefficients are given below.

$$A=\frac{1}{e}\cdot a_N S$$

$$p_0=k_c\sqrt{\frac{S_{\text{inj}}}{S}}(\cos\phi-\alpha\sin\phi)$$

$$q_2=a_N S+\frac{1}{\tau_n}-\left(g-\frac{1}{\tau_p}-a_S S\right)$$

$$q_1=a_N S(a_S S-g)-k_c^2\frac{S_{\text{inj}}}{S}-\left(g-\frac{1}{\tau_p}-a_S S\right)\cdot\left(a_N S+\frac{1}{\tau_n}+k_c\sqrt{\frac{S_{\text{inj}}}{S}}\cos\phi\right)$$

$$q_0=-k_c a_N\sqrt{S_{\text{inj}}\cdot S}(a_S S-g)(-\alpha\sin\phi+\cos\phi)-\left[\left(g-\frac{1}{\tau_p}-a_S S\right)k_c\sqrt{\frac{S_{\text{inj}}}{S}}\cos\phi+{k_c}^2\frac{S_{\text{inj}}}{S}\right]\cdot\left(a_N S+\frac{1}{\tau_n}\right)$$

where g is used for $G_0(N-N_0)/1+\epsilon S$, for simplicity. $a_N\ (=\partial g/\partial N)$ and $a_S\ (=\partial g/\partial S)$ are the differential gain of carriers and photon.

Compared with the ideal frequency response of a free running laser, which is a simple 2-pole response, the injection-locked response has a first- and third-order polynomial in the numerator and denominator, respectively. Not only will these enrich the characteristics of the frequency response, but also its resonance frequency, and damping are not well defined. This complicates the comparison of the follower laser S21 between various injection conditions.

Fortunately, since all of the coefficients p and qs are real, the S21 can only be of two forms: an over-damped response or an ideal 2-pole laser response accompanying with a parasitic pole (see Appendix). The over-damped response is not of interest and we will consider only the second case here. Recall that $\Omega=j\omega$, and the numerator of H will never be zero for any physical frequency; hence, it will only contribute a frequency-dependent scaling factor to the response. The third-order denominator will, therefore, determine the key S21 characteristics. Because the summation of these poles has to be real, there will be one real pole and two complex conjugated poles. The real pole will act like the parasitic pole in a parasitic-limited laser response, whereas the two conjugate poles will determine the resonance frequency and the damping of the injection-locked laser. The simulated S21 curve from (5) can, therefore, be fitted to the typical parasitic-limited frequency response [12]

$$|H'(f)|^2=\frac{1}{1+\left(\frac{f}{f_0}\right)^2}\cdot\frac{1}{\left(1-\left(\frac{f}{f_r}\right)^2\right)^2+\left(\frac{\gamma}{2\pi f_r}\right)^2\cdot\left(\frac{f}{f_r}\right)^2} \tag{6}$$

where f_0 is the parasitic pole frequency, f_r is the resonance frequency, and γ is the damping of the device. With this recognition, the follower laser S21 at various injection conditions can be meaningfully compared. This is extremely important for identifying the useful conditions within the huge injection-locking parameter space.

III. Analog Modulation

It has been demonstrated that by injection locking, the laser-resonance frequency can be increased up to three times its free running value [5]. The enhancement not only can potentially boost the laser performance for higher speed digital applications, but can also increase the SFDR for analog applications. We performed a thorough study of the laser-frequency response with various injection power and detuning conditions. Only those conditions that result in stable follower laser operation are measured and the Arnold tongue of the system can, thus, be mapped out. Conditions that result in phenomena such as chaotic behavior or frequency mixing are not considered "locked" and will not be studied. The impact of the polarization

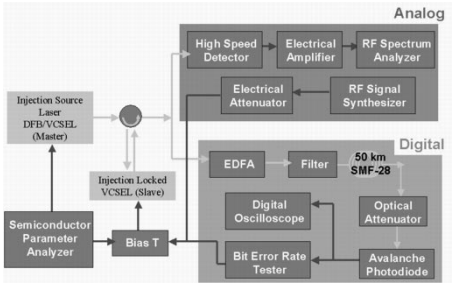

Fig. 1. Injection-locking setup for both digital and analog modulation.

of the injection light was also investigated and it does not seem to alter the general trend of the performance improvement. This is verified with several VCSELs are used in the experiment. In addition, the improvement of the SFDR can be realized in a relatively large-injection parameter space. This is extremely important for this technique to be practical. The third-harmonic SFDR of an 1.55-μm VCSEL was demonstrated to improve by 20 dB with injection locking to be 112 dB·Hz$^{2/3}$. This is, so far, the highest dynamic range for a long wavelength VCSEL.

A. Frequency-Response Enhancement

The schematic of the experimental setup is shown in Fig. 1. In this figure, the configurations for both digital and analog modulation are shown. A circulator is used to couple the light from the master DFB/VCSEL into the follower VCSEL. The follower lasers used in this experiment are directly modulated VCSELs around 1550 nm with a cantilever structure for wavelength tuning [13]. The output is monitored at the third port of the circulator.

Once the modulated follower VCSEL is stably locked, its frequency response is measured with a network analyzer at –10-dBm modulation power level. Fig. 2 shows family curves for various injection conditions. All of the S21 curves are fitted with (6) to obtain the resonance frequency and the damping values. In the case of a fixed detuning around 0 nm, the resonance frequency is enhanced more than 2 $\times$ for the strongest injection power. For a fixed injection power around 0 dBm, the resonance-frequency enhancement in Fig. 2(b) is more than 2 $\times$, but the damping clearly increases with the amount of detuning, resulting in both peaky and flat S21. A flat S21 is especially suitable for wideband-modulation applications. In some cases, the S21 are relatively flat from dc to 7 GHz, with resonance frequencies of more than 8 GHz. Compared to its free-running value at 3.5 GHz, this is a highly desirable improvement by injection locking.

Another interesting observation is that the amplitude of the S21 varies with different detuning values. This is clearly seen in the low-frequency regime, where the amplitude enhancement in Fig. 2(b) can be more than 10 dB in some cases for high detuning values. This improvement of the modulation efficiency directly translates into the RF gain in an analog link. The increase of the fundamental tone power also results in a larger spur-free dynamic range. This is another advantage of the injection-locking technique in the analog applications. The physical origin of this modulation-efficiency improvement is still under investigation.

The rich characteristics of the S21 curves warrant a thorough study for different injection conditions. S21 measurements

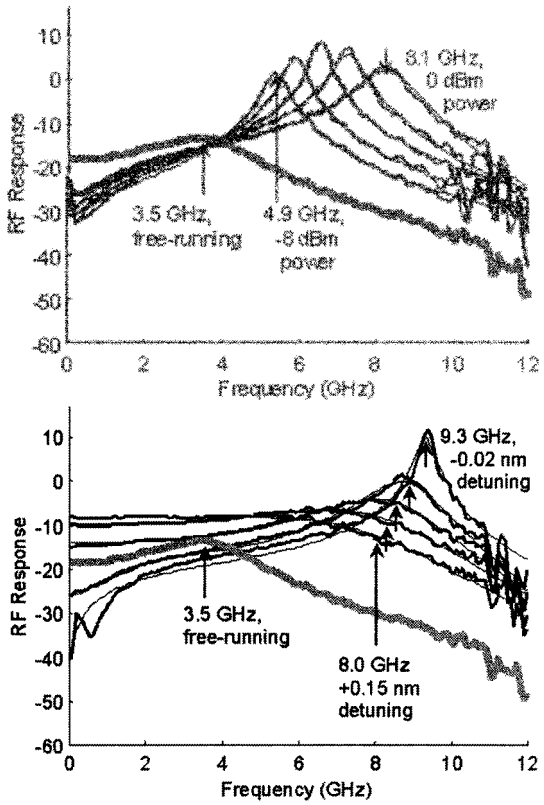

Fig. 2. Effect of injection power and detuning on frequency response. The free running S21 curve is also shown as the reference. The arrows indicate the position of the resonance peak from curve fitting. (a) For the fixed detuning case, the injection power is 0 dBm. (b) The resonance frequency increases with injection power. For the fixed injection power case, f_r increases from 8 to 9.3 GHz when detuning changes from $+0.15$ to -0.02 nm. The large detuning cases exhibit relatively flat S21 up to 7 GHz.

throughout the entire Arnold tongue were performed and the results were again curve-fitted to (6) to extract the resonance frequency and damping value. The obtained f_r and damping values are plotted against the injection power and detuning shown in Fig. 3.

Fig. 3(a) indicates that a higher resonance frequency can be achieved with a larger injection power. The injection power is defined as the absolute amount of power incident on the follower VCSEL, without taking into account the coupling loss. The small detuning values will result in a higher resonance frequency, but the effect is relatively small (note the almost-vertical stripes in the figure). From the damping Arnold tongue, it is obvious that both injection power and detuning play important roles in determining the damping value. The largest damping happens when both the injection power and detuning are large. The flattest S21 curve in Fig. 2(b) corresponds to the upper-right corner in the damping Arnold tongue. These two Arnold tongues suggest that a large positive detuning with a high injection power is the best for frequency response improvement.

The S21 simulation from (5) is also performed for the entire locking range. Similarly, the results are fitted with (6) to extract the S21 parameters. Fig. 4 shows the simulated Arnold tongue for the resonance frequency. In the simulation, the value of the x-axis (injection power ratio) is the product of the coupling coefficient and the square root of the master and follower power ratio. The value is proportional to the power that already pene-

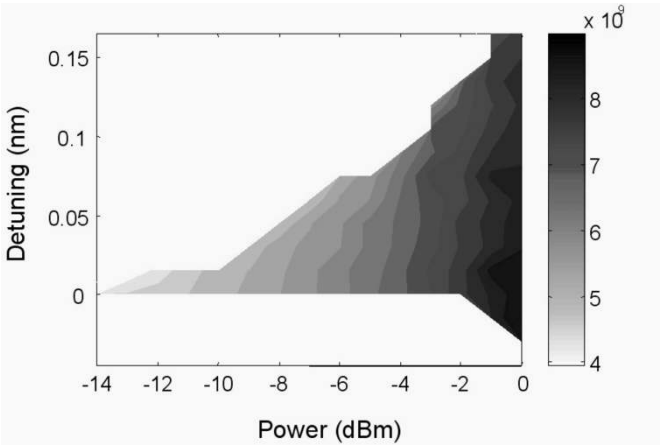

(a)

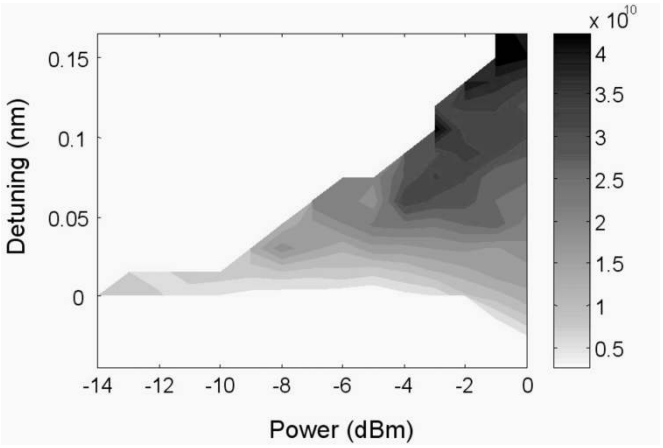

(b)

Fig. 3. Experimental Arnold tongues of resonance frequency and damping. Generally speaking, a higher injection power is always desirable to improve the resonance frequency.

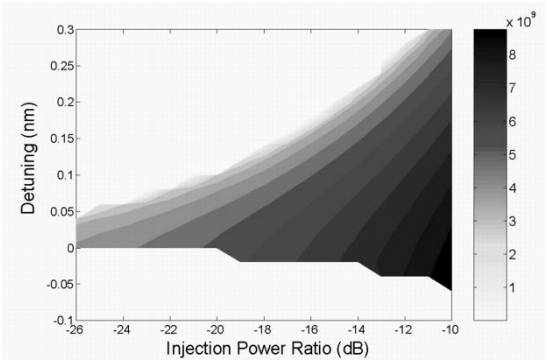

Fig. 4. Simulated Arnold tongues of resonance frequency. The theory predicts that the highest resonance frequency occurs at a high injection power and small detuning condition. Taking into account the difference in the definition of the injection power between the experiment and the simulation, the tilted stripes in the figure will become more vertical. The overall trend predicted by the theory matches well to the experimental Arnold tongue.

trates into the cavity and interacts with the follower laser field. This is different from the power injected onto the device used to plot the experimental Arnold tongues. Experimentally, we have observed that reflection coefficient varies with detuning relative to the cold-cavity resonance peak. In particular, the reflection coefficient is lowest at the cavity wavelength and increases

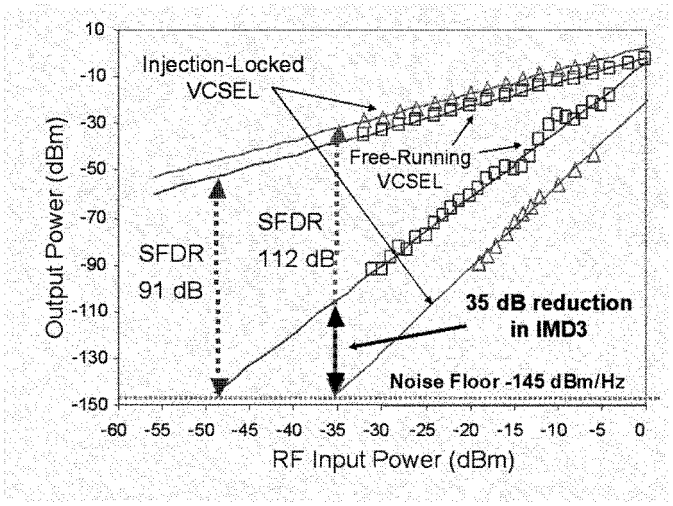

Fig. 5. Third-harmonic SFDR improvement with injection locking for an 1-GHz single-tone modulated VCSEL at 1538.4 nm. The incident DFB power is around -4 dBm with a detuning of $+0.24$ nm. SFDR is calculated with a RIN-limited system noise floor of -145 dBm/Hz. The increase in the fundamental tone accompanied with a decrease in the third-order harmonic distortion power enhanced the SFDR from 91 dB-Hz$^{2/3}$ to 112 dB-Hz$^{2/3}$.

as detuning increases; this results in a higher power coupling for 0-nm detuning. Note the similarity between Figs. 3(a) and 4. The figures would be even more similar if the theroretical power was calibrated to the actual power getting into the follower cavity (tilt the vertical strips in Fig. 4 to the left). The simulation shows that the resonance frequency can be enhanced with a stronger injection power and with a smaller detuning. The simulated-damping Arnold tongue (not shown) also shows that the highest damping occurs with a high injection power and large detuning. The theoretical predictions confirm the general trends observed experimentally.

B. SFDR Improvement

Nonlinear distortion of the transmitter is another important consideration for analog transmitters. It can be characterized by measuring either the second- or third-order harmonic distortion (for single-tone modulation) or the IMD3 (for two-tone modulation). In either case, spur-free dynamic range (SFDR) is the figure of merit of concern. It is defined as the dynamic range at the point when the system noise floor equals to the distortion power [14]. In our experiment, single-tone modulation is used to characterize the linearity of the VCSELs.

More than ten VCSELs were characterized in our experiments and all showed SFDR improvements with injection locking. The VCSELs were typically biased at approximately half of the peak power to maximize their useful linear range. Fig. 5 shows fundamental and third-harmonic power versus RF input power for one of the VCSELs at one particular injection condition at 1 GHz. A 5-dB enhancement of the fundamental tone power and a 35-dB reduction in the third harmonic distortion power were obtained with injection locking. The change in fundamental tone can be increased or decreased depending on detuning values, as shown in Fig. 2(b). The third-order SFDR is determined to be 91 and 112 dB-Hz$^{2/3}$ for the free running- and injection-locked cases, respectively. This results in the record 112-dB-Hz$^{2/3}$ SFDR value for the long-wavelength

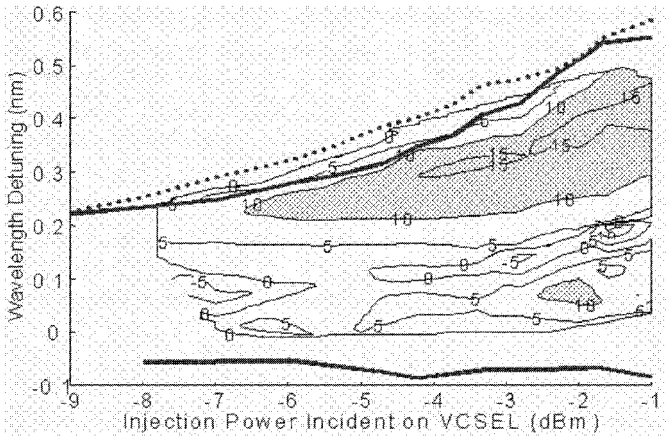

Fig. 6. Third harmonic SFDR improvement. The shaded area corresponds to the case when improvement is larger than 10 dB. The plot shows an improvement of SFDR between 0.2 and 0.5 nm detuning. This large detuning tolerance makes the injection-locking technique attractive in a practical system.

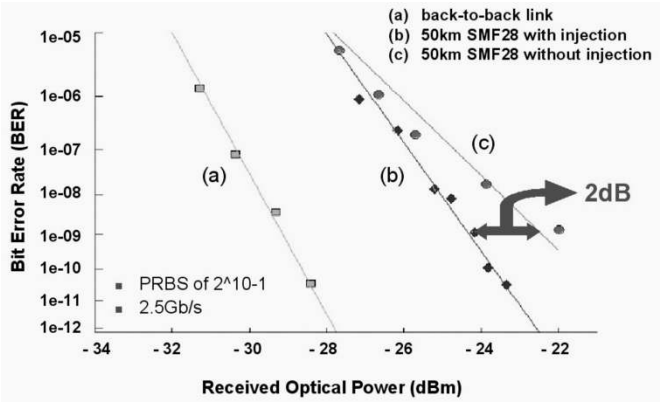

Fig. 7. BER versus received power for different conditions. Note the improvement after transmission through fiber when the VCSEL is injection-locked.

VCSELs. The system noise floor of −145-dBm/Hz originates from the relative intensity noise (RIN) of the VCSEL.

The reasons for the observed SFDR improvements can be understood as follows: nonlinear distortion is reduced because injection locking increases the resonance frequency. A larger offset between the modulation and resonance frequencies reduces the carrier-photon interaction, which in turn reduces the third-harmonic distortion. Also in Fig. 2(b), we observed an increase in the amplitude of the frequency response at certain frequencies for some injection conditions. The combination of the two effects results in a larger SFDR.

Improvements of fundamental tone power as high as 8 dB were observed with high optical injection power. It is possible that even higher injection powers would further increase the RF fundamental tone power. For the third-harmonic distortion, the highest reduction observed in the vicinity of the fundamental tone power increase peak was 40 dB. The maximum reduction occurs at roughly −5-dBm injection power.

It appears that higher optical injection powers reduce the improvement in harmonic distortion. The highest fundamental tone increase and the greatest third-harmonic reduction do not occur at the same injection condition (different detuning and injection power values). Hence, the maximum third-order SFDR will occur at a point between the two respective maxima. From Fig. 6, the greatest estimated SFDR improvement at this RF input power was 17 dB. The actual SFDR improvement value is sensitive to the slope of the line. This explains why we actually observed a ∼20-dB-Hz$^{2/3}$ improvement in Fig. 5. The shaded area in Fig. 6 represents the conditions when the SFDR improvement is more than 10 dB-Hz$^{2/3}$. This implies that the injection parameters do not have to be precise in order to obtain reasonable improvement. This is important for this technique to be useful in a practical system.

IV. Digital Modulation

For digital modulation applications, all injection-locking experiments so far used DFB lasers as the master source. The injection conditions in those experiments were all in the strong injection regime. In our study, a VCSEL is used as the master source and its output power is only 30 μW. We demonstrated that even with a weak injection power, chirp reduction can still be achieved. This low-power requirement implies that a high-power master laser could be used directly to simultaneously lock and improve the performance of several transmitters.

A. BER Measurement

The experimental setup is shown in Fig. 1. The BER of the VCSEL directly modulated at 2.5 Gb/s is plotted against the received optical power in Fig. 7. Line (a) represents the signal from the follower VCSEL directly coupled to the APD without fiber and without injection locking. Lines (b) and (c) correspond to the transmission performance of the follower VCSEL through 50 km of SMF-28 fiber, with and without injection, respectively. Line (c) shows a power penalty in transmission and a shallower slope compared to the reference line (a). The reduction of the slope is likely due to the interaction of the chirp of the directly modulated VCSEL (linewidth-enhancement factor $\sim$5) and the fiber (dispersion 17 ps/nm·km for SMF-28 fiber). For the eyediagrams measured at the same received power, the eye in the free running condition has a large spreading of the signal traces at the rising edge, compared with the one when the follower laser is injection locked.

B. Chirp Reduction

To verify that chirp reduction is the reason for the performance improvement, an Advantest dynamic chirp measurement system was used to measure the real time wavelength information of the signal, for both free-running and injection-locked cases. For this experiment, another tunable 1550-nm VCSEL is used as the follower laser while a DFB laser serves as the master.

Fig. 8 shows the chirp of the follower VCSEL with and without injection. For both cases, the VCSEL is modulated with the same waveform. In a directly modulated laser, frequency chirp depends on the modulation format and the linewidth-enhancement factor of the laser. For high-speed modulation, the transient chirp usually dominates and is around 7.8 GHz in this case. The adiabatic chirp is also obvious. When the laser is injection locked [Fig. 8(b)], both the transient and adiabatic chirp is effectively reduced.

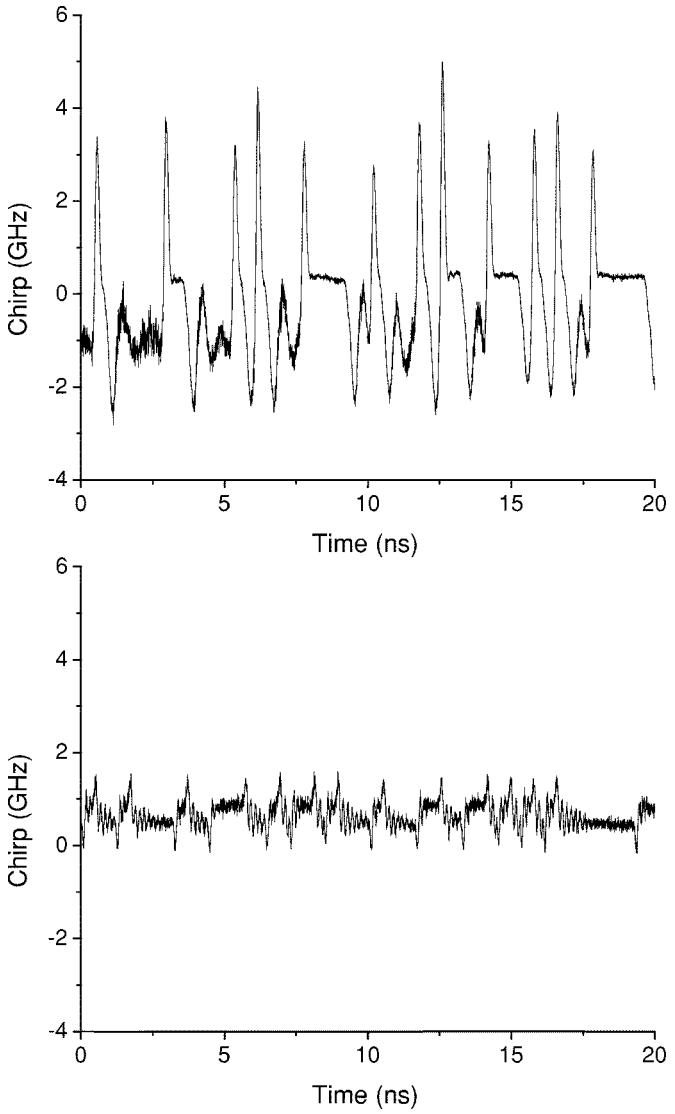

Fig. 8. (a) Chirp of the modulated VCSEL for the cases of free-running and injection locked. The transient chirp 7.8 GHz dominates in the free-running case. (b) The VCSEL is locked to a 8-dBm, +0.025-nm detuned DFB. Both the transient and adiabatic chirp are drastically reduced.

C. Simulation

The injection-locked chirp can also be derived from (1) as follows

$$\frac{d\phi}{dt} = \frac{\alpha}{2}\frac{\epsilon S}{\tau_p} + \frac{\alpha}{2}\frac{1}{S}\frac{dS}{dt} - \Delta\omega + k_c\sqrt{\frac{S_{\text{inj}}}{S}}\left[\sin\left(\Delta\phi(t)\right) - \alpha\cos\left(\Delta\phi(t)\right)\right]. \quad (7)$$

The first term, the adiabatic chirp, corresponds to the change of frequency for different current densities. The second term is the transient chirp. It dictates the wavelength variation based on how the photon number is modulated and, in the case of digital modulation, is the dominant term. Transient chirp remains one of the most challenging issues in deploying 10 or 40 Gb/s directly modulated lasers systems. The other terms are the effect of injection locking. They offer a possibility to cancel both the adiabatic and transient chirp in a modulated laser. The detuning contributes to a constant wavelength shift and can be either positive or negative.

With (1), digital-modulation performance of the follower laser can be simulated. First, the amplitude and phase of the master laser are solved at a given bias level. This information is then fed into the injection-locking rate equations to calculate the dynamics of the follower laser. The frequency detuning and the injection efficiency are specified independent from the device parameters.

The simulated chirp and eye-diagrams at 2.5 Gb/s match well with our experimental results, which encourages us to investigate the simulation at a higher speed. BER plots also match in trend the reduction in power penalty. In a 10-Gb/s system, the chirp of a directly modulated laser is even more severe. The peak-to-peak transient chirp is now more than 20 GHz and the resultant eye is seriously distorted after 50 km of SMF-28 fiber. With a proper injection condition, chirp is effectively eliminated and the eye is fully open. This indicates that the injection locking technique can be very useful when the laser is directly modulated at 10 Gb/s or above.

V. Novel Uncooled Application

The wavelength in current dense wavelength division muliplexed (DWDM) transmitters varies with temperature. This necessitates accurate temperature control as well as a wavelength-stabilization system to ensure that each laser operates on the DWDM grid. The wavelength stabilizer is typically implemented with Fabry-Perot etalon and a thermal-electric temperature controller, which increases cost, power consumption, and size. Uncooled DWDM-grid transmitters are, thus, extremely attractive for systems involving a high number of low-cost transmitters, such as fiber-to-the-home.

A stable master laser can lock and stabilize the follower laser to the correct wavelength, and provide a performance improvement. For the tunable VCSELs used in our experiments, the laser wavelength can be independently controlled by the cantilever tuning voltage. With the VCSEL uncooled we adjust its lasing wavelength with the proper tuning voltage for the given ambient temperature. Since the locking range is usually several Å, accuracy of the tuning voltage can be further relaxed. As long as the VCSEL is tuned, such that the detuning between the two lasers is within the locking range, its wavelength will match to the master source wavelength.

A. Experiment

In our study on the temperature effects, the VCSEL was temperature controlled from 20 °C to 50 °C to simulate the possible ambient temperature drift. Its bias is chosen at 5 mA, which gives a peak power for the VCSEL at 50 °C. The DFB is at 100 mA for a lasing wavelength of 1545.15 nm. When the ambient temperature is changed, the DFB bias, the VCSEL bias, and its modulation amplitude all remain the same. Only the VCSEL cantilever tuning voltage is adjusted to achieve the desired wavelength detuning and performance improvement.

The IMD3 SFDR with two tones at 990 MHz and 1 GHz is first measured when the DFB is off to serve as the free-running reference. For each injection condition, measurements are

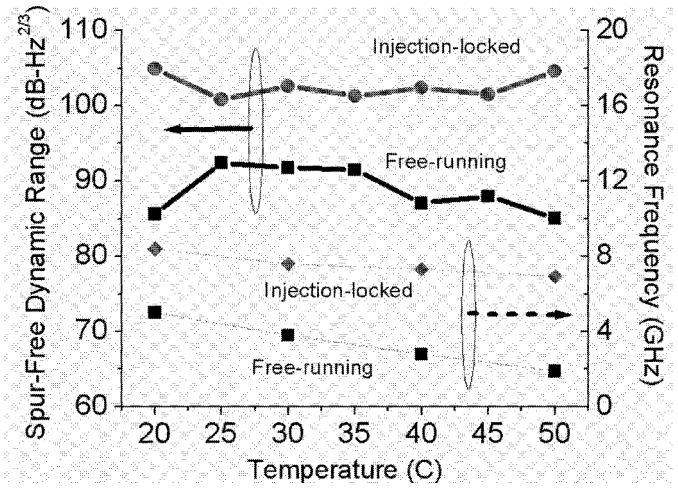

Fig. 9. IMD3 SFDR and resonance frequency at various temperatures for both free-running and injection-locked cases. The modulation frequencies are at 990 MHz and 1 GHz for the SFDR measurement. The injection-locked SFDR is always better than the free-running case, provided that a proper detuning is chosen. A constant enhancement of the resonance frequency is observed throughout the measured temperature range as well.

performed and compared with the free-running references. In Fig. 9, the injection-locked resonance frequency and the SFDR of various temperatures are shown. The free-running SFDR degrades with higher temperature, while the best-case injection-locked SFDR remains reasonably uniform between 92–97 dB-Hz$^{2/3}$, with an improvement ranging from 8 to 20 dB-Hz$^{2/3}$. Note that the resonance-frequency enhancement is rather insensitive to the temperature change. The injection-locked resonance frequency remains reasonably uniform around 7.5 GHz over the temperature range, showing an improvement for most of the cases.

Note that this particular wavelength was chosen for a large temperature tuning range rather than for an optimal SFDR at a particular temperature. Higher SFDR values and improvements can indeed be achieved for different wavelengths. For example, an injection-locked SFDR value of 108 dB-Hz$^{2/3}$ was observed at 15 °C with a wavelength of 1543.5 nm.

B. Proposed System Architecture

Using the injection-locking technique to compensate for the wavelength drift and performance degradation of temperature, it is possible to use one master laser to simultaneously lock several different DWDM transmitters as shown in Fig. 10. Recently, a semiconductor mode locked laser at 1.55 μm has been demonstrated to have a very stable amplitude and phase relation between different modes [15]. The mode spacing for the mode-locked laser could be designed to match a chosen WDM channel wavelength spacing, and the laser be used as the injection source. Alternatively, one can use an optical frequency comb generator [16] as the master laser. As shown in the proposed architecture, the output of the master is sent into a demultiplexer following a circulator, and feeds into lasers at different channels, similar to our experimental setup. If the master injection source has a stable output, this 1-N injection-locking architecture will have a similar performance as to the experiment, where each follower laser is injection-locked by its own master

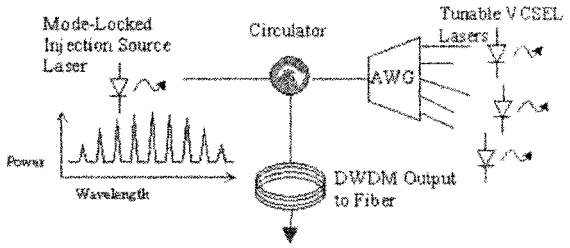

Fig. 10. Proposed-system architecture for uncooled injection-locked transmitters at different WDM grid. The master output is coupled into an arrayed waveguide grating (AWG), which filters out only one wavelength component from the master, through a circulator. The filtered master field locks the uncooled tunable VCSELs to the ITU grid and improves their performances. The signal from each follower VCSEL is then coupled back to AWG, aggregated and sent to output fiber through the circulator.

laser. The removal of the wavelength stabilizer in each transmitter, which drastically simplifies the module cost and size, with the additional performance improvement makes this architecture extremely attractive.

VI. Conclusion

The frequency response of an injection-locked laser was found to be the same as that of a parasitics-limited laser. It is therefore possible to describe the follower laser frequency response with resonance frequency and damping, similar to an ideal two-pole response. The theory matches well with our thorough measurement throughout the entire locking range. We pointed out that a high injection power and detuning value is promising to achieve a flat S21 with a high resonance frequency. When the follower laser is injection locked, the enhancement of the fundamental tone power and the reduction of the nonlinear distortion drastically improve the spur-free dynamic range in the analog applications. For digital modulation, chirp reduction by injection locking improves the BER performance. The technique can be especially useful when the system speed exceeds 10 Gb/s. Finally, we demonstrated a novel application of injection-locking with an uncooled tunable VCSEL. A novel architecture was also proposed to use one master laser to simultaneously lock many follower lasers at different DWDM channels. The idea has the potential to reduce the size and cost of the transmitter modules tremendously.

Appendix I
Frequency Response of Injection-Locked Lasers

Consider the third-order injection locking frequency response, (5). As discussed previously, the locations of the poles will determine the characteristics of the S21. Note that the coefficients q_i are real and q_2 and q_3 are negative for typical laser parameters. These restrictions limit the possible pole configurations to those shown in Fig. 11. In this figure, increasing the frequency ω corresponds to moving along the positive imaginary axis. The amplitude of the frequency response is the reciprocal of the product of all the distances from the physical frequency to the poles. Thus, the first situation, where all of the poles are on the real axis, represents the over-damped condition. For the case on the right, it resembles the situation of a parasitics-limited laser. The two conjugate poles determine

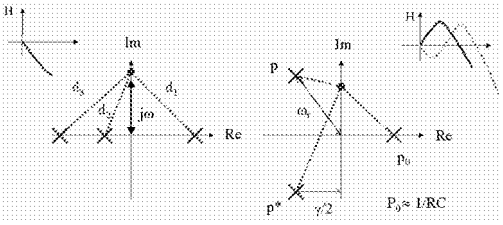

Fig. 11. Poles of an injection-locking system. Due to the limitation on the coefficients, only the above two configurations need to be considered. The left situation where all the poles are on the real axis corresponds to an over-damped frequency response. When the physical frequency increases (moving along the positive imaginary axis), the product of d_1, d_2, and d_3 increases monotonically. The resulting amplitude of the frequency response, therefore, monotonically decreases with higher frequency. The situation on the right is the same as that of a parasitic-limited laser. Depending on the value of p_0, the response may be close to an ideal laser or suffers dips in the low-frequency regime.

the resonance frequency and the damping while the position of the third pole determines whether there will be a dip before the resonance peak in the frequency response.

ACKNOWLEDGMENT

The authors would like to thank Dr. R. Stone, Dr. J. Boucart, and Dr. W. Yuen at Bandwidth9 Inc. for providing the VCSELs and some of the equipment used in the experiments, as well as for their invaluable input.

REFERENCES

[1] Y. Yamamoto and T. Kimura, "Coherent optical fiber transmission systems," *IEEE J. Quantum Electron.*, vol. QE-17, pp. 919–935, June 1981.

[2] P. Gallion, H. Nakajima, G. Debarge, and C. Chabran, "Contribution of spontaneous emission to the linewidth of an injection-locked semiconductor laser," *Electron. Lett.*, vol. 22, pp. 626–628, 1985.

[3] K. Iwashita and K. Nakagawa, "Suppression of mode partition noise by laser diode light injection," *IEEE J. Quantum Electron.*, vol. QE-18, pp. 1669–1674, Oct. 1982.

[4] N. A. Olsson, H. Temkin, R. A. Logan, L. F. Johnson, G. J. Dolan, J. P. Van der Ziel, and J. C. Campbell, "Chirp-free transmission over 82.5 km of single mode fibers at 2 Gbit/s with injection locked DFB semiconductor lasers," *IEEE J. Lightwave Technol.*, vol. LT-3, pp. 63–67, Feb. 1985.

[5] X. Meng, T. Chau, and M. C. Wu, "Experimental demonstration of modulation bandwidth enhancement in distributed feedback lasers with external light injection," *Electron. Lett.*, vol. 34, no. 21, pp. 2031–2032, 1998.

[6] R. Lang, "Injection locking properties of a semiconductor laser," *IEEE J. Quantum Electron.*, vol. QE-18, pp. 976–983, June 1982.

[7] N. Schunk and K. Petermann, "Noise analysis of injection-locked semiconductor injection lasers," *IEEE J. Quantum Electron.*, vol. QE-22, pp. 642–650, May 1986.

[8] L. A. Coldren and S. W. Corzine, *Diode Lasers and Photonics Integrated Circuits*: Wiley, 1995.

[9] C. H. Henry, N. A. Olsson, and N. K. Dutta, "Locking range and stability of injection locked 1.54-μm InGaAsP semiconductor lasers," *IEEE J. Quantum Electron.*, vol. QE-21, pp. 1152–1156, Aug. 1985.

[10] A. Pikovsky, M. Rosenblum, and J. Kurths, *Synchronization: A Universal Concept in Nonlinear Science*. Cambridge, U.K.: Cambridge Univ. Press, 2001.

[11] I. Petitbon, P. Gallion, G. Bebrarge, and C. Chabran, "Locking bandwidth and relaxation oscillations of an injection-locked semiconductor laser," *IEEE J. Quantum Electron.*, vol. 24, pp. 148–154, Feb..

[12] B. J. Thibeault, K. Bertilsson, E. R. Hegblom, E. Strezelecka, P. D. Floyd, R. Naone, and L. A. Cildren, "High-speed characteristics of low-optical loss oxide-apertured vertical-cavity lasers," *IEEE Photon. Technol. Lett.*, vol. 9, pp. 11–13, Jan. 1997.

[13] G. S. Li, R. F. Nabiev, W. Yuen, M. Jasen, D. Davis, and C. J. Chang-Hasnain, "Electrically-pumped directly-modulated tunable VCSEL for metro DWDM applications," in *Proc. Eur. Conf. Opt. Commun.*, vol. 12, Amsterdam, The Netherlands, 2001, pp. 1686–1688.

[14] R. V. Dalal, R. J. Ram, R. Helkey, H. Roussell, and K. D. Choquette, "Low distortion analogue signal transmission using vertical cavity lasers," *Electron. Lett.*, vol. 34, no. 16, pp. 1590–1591, 1998.

[15] C. M. Depriest, T. Yimaz, P. J. J. Delfyett, S. Etemad, A. Braun, and J. Abeles, "Ultralow noise and supermode suppression in an actively mode-locked external-cavity semiconductor diode ring laser," *Opt. Lett.*, vol. 27, no. 9, pp. 719–721, 2002.

[16] C. F. C. Silva, A. J. Seeds, and P. J. Williams, "Terahertz span >60-channel exact frequency dense WDM source using comb generation and SG-DBR injection-locked laser filtering," *IEEE Photon. Technol. Lett.*, vol. 13, pp. 370–372, Apr. 2001.

Chih-Hao Chang (S'99) was born in Taipei, Taiwan, in 1973. He received the B.S. degree from National Taiwan University, Taipei, Taiwan, in 1995 and the Ph.D. degree from the University of California, Berkeley in 2002, both in electrical engineering.

During 1995–1997, he served in the Chinese Army. His research interests include high-speed vertical cavity surface emitting lasers, dynamics of injection locking, and WDM systems.

Lukas Chrostowski (S'98) was born in Warsaw, Poland, in 1975. He received the B.Eng. degree in electrical engineering from McGill University, Montreal, Canada, in 1998. He is currently pursuing the Ph.D. degree at the University of California, Berkeley.

His research interests include injection locking of vertical cavity surface emitting lasers (VCSEL) for high-speed analog and digital modulation, VCSEL characterization, design and modeling, and WDM systems.

Connie J. Chang-Hasnain (M'88–SM'92–F'98) received the B.S. degree from the University of California, Davis, in 1982 and the M.S. and Ph.D. degrees from the University of California, Berkeley, in 1984, and 1987, respectively, all in electrical engineering.

She was a Member of Technical Staff at Bellcore from 1987 to 1992. From April 1992 to December 1995, she was an Associate Professor of Electrical Engineering at Stanford University, Stanford, CA. Since January 1996, she has been a Professor in the Department of Electrical Engineering, University of California, Berkeley. She founded BANDW1DTH9 Inc., Fremont, CA, in 1997, and served as its Chairman, President, and CEO from 1997 to 2000. Her research interests have been in the area of semiconductor optoelectronic devices, with a particular focus on wavelength-engineered vertical cavity lasers and detectors and novel systems applications. She has authored over 200 papers in leading technical journals and conferences, six book chapters, and has presented over 100 invited talks. She holds 18 patents.

Dr. Chang-Hasnain is a Fellow of the Optical Society of America (OSA), a Presidential Faculty Fellow, a Packard Fellow, a Alfred P. Sloan Research Fellow, and a National Young Investigator. She was an Editor of the IEEE CIRCUITS AND DEVICES Magazine and Guest Editor of the IEEE JOURNAL ON SELECTED TOPICS ON QUANTUM ELECTRONICS Special Issue on Semiconductor Lasers in 1998. She served as General Chair of the 1999 Conference on Lasers and Electro-Optics (CLEO) and as the Conference Chair of the first VCSEL Conference in 1997. She was a Member of the Lasers and Electro-Optics Society (LEOS) Board of Governors during 1992–1995, a member of the U.S. Air Force Scientific Advisory Board during 1997–1999, and is a current Member of the Board of Directors of the OSA. She was named the Outstanding Young Electrical Engineer by Eta Kappa Nu in 1992. She received the 1994 Distinguished Lecturer Award of IEEE LEOS and the 1999 Curtis W. McGraw Research Award from the American Society of Engineering Education.